Desalination and Water Treatment
www.deswater.com
doi: 10.1080/19443994.2014.895777

54 (2015) 1990–1997
May

Taylor & Francis
Taylor & Francis Group

Adsorption behavior of Lanthanum(III) on SQD-85 resin

Leilei Pi[a], Chunhua Xiong[a,*], Jianxiong Jiang[b], Xuming Zheng[c], Feiyan Chen[a], Caiping Yao[a], Qunxiong Zheng[a]

[a]*Department of Applied Chemistry, Zhejiang Gongshang University, No. 149 Jiaogong Road, Zhejiang, Hangzhou 310012, China, Tel. +86 571 88071024 7571, +86 13357196703; email: xiongch@163.com*
[b]*Key Laboratory of Organosilicon Chemistry and Material Technology of Ministry of Education, Hangzhou Normal University, Zhejiang, Hangzhou 310012, China*
[c]*Engineering Research Center for Eco-Dyeing & Finishing of Textiles, Ministry of Education, Zhejiang Sci-Tech University, Zhejiang, Hangzhou 310018, China*

Received 2 August 2013; Accepted 11 February 2014

ABSTRACT

The adsorption and desorption behaviors of La(III) on SQD-85 resin were investigated using batch and column methods. Batch adsorption studies were carried out with different pH, contact time, and temperature. In the batch system, the SQD-85 resin exhibited the highest La(III) uptake as 478 mg/g at 308 K, at an initial pH value of 6.5. The adsorption of La(III) follows the Langmuir isotherm better than Freundlich isotherm. The thermodynamic parameters such as the positive value of ΔH showed that the adsorption was endothermic in nature and ΔG, which were all negative, indicated that the adsorption of La(III) ions onto SQD-85 resin was spontaneous. Column adsorption experiments indicated the maximum adsorption capacity of 481 mg/g for La(III), and Thomas model was applied to experimental column data to determine the characteristic parameters of column useful for process design. The desorption rate of La(III) was 99.8% when the elution agent is 1.0 mol/L HCl solution. These results suggest that La(III) in aqueous solution can be removed and recovered by SQD-85 resin efficiently.

Keywords: SQD-85 Resin; La(III); Adsorption; Desorption; Kinetics; Thermodynamics

1. Introduction

Rare earth elements are being increasingly used as important components in national defense industry, metallurgy, machinery, chemical industry, agricultural, and pastoral farming for their unusual spectroscopic characteristic [1–4]. The lanthanide series of elements comprises the elements between lanthanum in the periodic table of elements. From the lanthanide elements, lanthanum, the first rare earth element, has attracted increasing interests to its unique physical and chemical properties because of increasing demands for advanced new materials. Lanthanum is usually applied for advanced new materials such as super alloys, catalysts, special ceramics, and organic synthesis [5,6]. Lanthanum can enter the environment in large quantities and is known to accumulate in the human body when inhaled or digested from food chain.

Several techniques, such as ion exchange, chemical precipitation, membrane separation, reverse osmosis, and extraction chromatography have been reported

*Corresponding author.

for the adsorption and separation of rare earth elements from aqueous solution [7–11]. Compared with other methods, ion exchange has received considerable attention in recent years because it is simple, convenient, effective in removing metal ions, relatively low cost and environmentally friendly [12–14]. SQD-85 resin (macroporous weak acid cation exchange resin, acrylic acid as polymer matrices) is milky white polymeric particle that the degree of cross-linking is 12%, specific surface area is 540–580 m^2/g, and average pore diameter is 12–16 nm. It contains a functional group (–COOH), and not only has the proton that can exchange with cation, but also has oxygen atom that can coordinate directly with metal ions [15]. Its principal characteristics are great chemical and physical stability, high exchange capacity, good regeneration ability, and it is commercially produced, so it can be widely available to remove metals from water and industrial wastewater. Due to above-mentioned properties SQD-85 resin has been preferred in this study.

In the present work, batch and column experiments were performed to test the feasibility of removal and recovery of La(III) from aqueous solution by using the SQD-85 resin. The adsorption mechanism of SQD-85 resin for La(III) ion is examined by infrared spectrometry and chemical analysis. SQD-85 resin is expected to be an excellent adsorption material with large adsorption capacity and high elution rate. The experimental results also provide theoretical basis for concentration of La(III) in analytical chemistry and extraction of La(III) in hydrometallurgy.

2. Materials and methods

2.1. Apparatus

The concentration of La(III) was measured by means of spectrochemical analysis colored by Arsenazo I using Shimadzu UV-2550 UV–vis spectrophotometer. Mettler toledo delta 320 pH meter was used for measuring pH of solutions. The sample was shaken in DSHZ-300A and THZ-C-1 temperature constant shaking machine. The water used in the present work was purified using Molresearch analysis-type ultrapure water machine. The IR spectra were recorded on a Nicolet 380 FTIR spectrometer.

2.2. Material

SQD-85 resin was supplied by Jiangsu Suqing Water Treatment Engineering Group and the properties are shown in Table 1. Stock solutions of La(III) ion were prepared from its oxides via dissolution in concentrated hydrochloric acid. HAc–NaAc buffer solution with pH 5.5–7.0 and $C_6H_{15}O_3N$–HNO_3 buffer solution with pH 7.20 were prepared from the NaAc, HAc, $C_6H_{15}O_3N$, and HNO_3 solutions. The chromophoric reagent of 0.1% Arsenazo I solution was obtained by dissolving 0.1000 g Arsenazo I powder into 100 mL purified water. All other chemicals were AR grade.

2.3. Adsorption experiments

Experiments were run in a certain range of pH, temperature, and contact time. The operations for the adsorption and desorption of La(III) were carried out in glass vessels and glass columns.

Batch experiments were performed under kinetics and equilibrium conditions. A desired amount of treated SQD-85 resin was weighed and added into a conical flask, followed by the addition of a desired volume of buffer solution with desired pH value. After 24 h, a required amount of standard solution of La(III) was put in. The flasks were shaken in a shaker at constant temperature and rotation speed. The upper layer of clear solution was taken for analysis until adsorption equilibrium reached.

In the column experiments, continuous packed bed studies were performed in a fixed bed mini glass column of 0.3 cm inner diameter with SQD-85 resin and filled with the La(III) solution that was fed from the top at a fixed flow rate. The La(III) solutions at the outlet of the column were collected at regular time intervals and the concentrations of La(III) were measured till the outlet and inlet concentrations became equal.

2.4. Analytical method

A solution containing a required amount of La(III) was added into a 25 mL colorimetric tube, and then 1.0 mL of 0.1% Arsenazo I solution and 10 mL pH 7.20 $C_6H_{15}O_3N$–HNO_3 buffer solution were added, after the addition of purified water to the mark of the color-

Table 1
General description and properties of SQD-85 resin

Items	Properties
Functional group	–COOH
Mass capacity (mmol/g)	≥10.5
Moisture (%)	50–60
Wet superficial density (g/mL)	0.70–0.80
True wet density (g/mL)	1.10–1.20
Particle size (≥95%)	0.315–1.25 mm
Whole bead after osmotic attrition	≥90

imetric tube, the absorbency was determined in a 1 cm colorimetric vessel at wavelength of 572 nm and compared with blank test. The adsorption capacity (Q, mg/g) and distribution coefficient (D, mL/g) were calculated with the following equations [16]:

$$Q = \frac{C_0 - C_e}{m} V \quad (1)$$

$$D = Q/C_e \quad (2)$$

where C_0 is initial concentration in solution (mg/mL); C_e is equilibrium concentration in solution (mg/mL); V is volume of solution (mL); m is dry weight of resin (g).

3. Results and discussion

3.1. Influence of pH on distribution coefficient for La(III) ion

Adsorption property is dependent on the pH of the solution which affects the surface charge of adsorbents, the degree of ionization and species of adsorbate. The influence of pH on the sorption behaviors of SQD-85 resin for La(III) is shown in Fig. 1. The results indicate that the adsorption capacity of La(III) was the highest when pH was 6.5 in the HAc–NaAc medium and decreased by either raising or lowering pH under the experimental condition.

The La(III) uptake can increase as the pH went up, and it can be explained based on a decrease in competition between H^+ ion and La(III) ion for the same adsorption sites. Beyond pH 6.5, due to the formation of suspended gelatinous lanthanides hydroxides, the adsorption of La(III) ions is reduced [17]. The subsequent adsorption experiments were carried out at pH 6.5 in HAc–NaAc system.

3.2. Determination of adsorption rate constant

The influence of contact time on the adsorption of La(III) onto SQD-85 resin (Fig. 2) was investigated at 288, 298, and 308 K. As shown, the amount of adsorption increased with increasing contact time, and the maximum adsorption was observed after 40 h, beyond which there was almost no further increase in the adsorption. In addition, the maximum adsorption capacities increased with increase in the temperatures, and the highest La(III) uptake capacity is 478 mg/g at 308 K.

Adsorption kinetics curves were obtained for La (III) on SQD-85 resin. The kinetics of adsorption can be described by the liquid film diffusion model [18], using the Brykina method [19]:

$$-\ln(1 - F) = kt \quad (3)$$

where F is the fractional attainment of equilibrium ($F = Q_t/Q_e$), where Q_e and Q_t are the amounts of La(III) adsorbed on the adsorbent at equilibrium at various times, respectively; k is the adsorption rate constant.

The experimental results accorded with the equation and a straight line was obtained by plotting $-\ln(1-F)$ vs. t. The results were listed in Table 2. According to the Boyd equation, it can be deduced from the linear relationship of $-\ln(1-F)$ vs. t that the liquid film diffusion was the predominating step of the adsorption process.

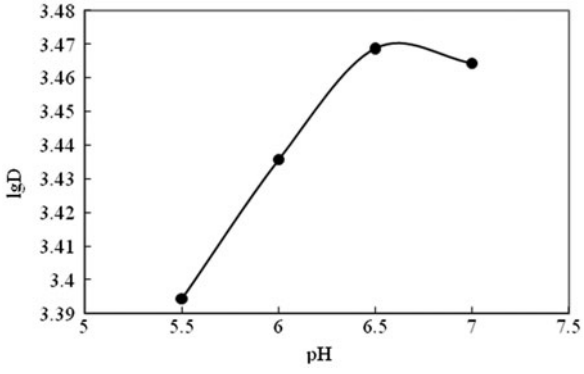

Fig. 1. Influence of pH on the distribution coefficient (resin 15.0 mg, 298 K, 100 rpm, and C_0 = 10 mg/30.0 mL).

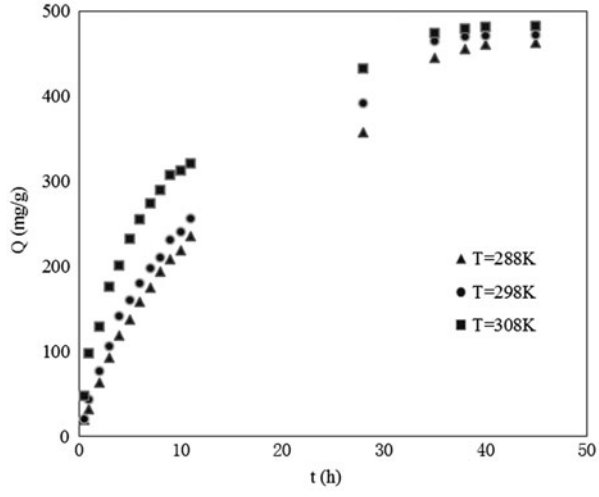

Fig. 2. Adsorption amount of different temperatures (resin 30.0 mg, pH 6.5, 100 rpm, and C_0 = 20.0 mg/60.0 mL).

Table 2
Adsorption rate constants

T (K)	Linearity relation of $-\ln(1-F)$ and t	$k \times 10^{-5}$ (s^{-1})	R^2
288	$y = 0.067x + 0.012$	1.86	0.997
298	$y = 0.075x + 0.020$	2.08	0.994
308	$y = 0.114x + 0.092$	3.16	0.991
318	$y = 0.314x + 0.155$	8.72	0.988

3.3. Adsorption isotherms

The adsorption isotherm studies are of fundamental importance in determining the adsorption capacity of La(III) onto SQD-85 resin and it diagnoses the nature of adsorption. The Langmuir and Freundlich isotherm models were used to interpret equilibrium isotherm data.

The Langmuir isotherm is based upon an assumption of monolayer adsorption onto a surface containing a finite number of adsorption sites of uniform energies of adsorption with no transmigration of adsorbate in the plane of the surface. The Langmuir isotherm is governed by the following relationship [20]:

$$\frac{C_e}{Q_e} = \frac{1}{Q_o K_L} + \frac{C_e}{Q_o} \tag{4}$$

where Q_e and C_e are the equilibrium concentration of La(III) on adsorbent and in solution, respectively, Q_o is the maximum adsorption capacity corresponding to complete monolayer coverage (mg/g), and K_L is the Langmuir constant and related to the free energy of adsorption.

The Freundlich isotherm model assumes heterogeneous surface energies in which energy term in Langmuir equation varies as a function of surface coverage. The Freundlich isotherm equation is used in the general form, as shown below [21]:

$$\lg Q_e = \frac{1}{n}\lg C_e + \lg K_F \tag{5}$$

where K_F and n are the Freundlich isotherm constants related to adsorption capacity and intensity of adsorption, respectively.

The Langmuir and Freundlich parameters for the adsorption of La(III) ion onto SQD-85 resin are listed in Table 3. From the better correlation coefficient and the fact that the equilibrium adsorption capacities (Q_o) obtained from Langmuir isotherm model are close to the experimentally observed saturation capacities, it can be concluded that the monolayer Langmuir adsorption isotherm is more suitable to explain the adsorption of La(III) onto SQD-85 resin.

3.4. Thermodynamic parameters

Both energy and entropy considerations in any adsorption procedure should be taken into account, in order to determine which process will take place spontaneously. Values of thermodynamic parameters are the actual indicators for practical application of a process. The amounts of La(III) adsorbed at equilibrium at 288, 298, and 308 K have been examined to obtain thermodynamic parameters for the adsorption system.

Thermodynamic parameters, such as changes in the Gibbs free energy (ΔG), enthalpy (ΔH), and entropy (ΔS) associated to the adsorption process, were determined using the following equations [22]:

$$\lg K_L = -\frac{\Delta H}{2.303RT} + \frac{\Delta S}{2.303R} \tag{6}$$

$$\Delta G = \Delta H - T\Delta S \tag{7}$$

where R is the gas constant and T is the absolute temperature.

As can be observed in Fig. 3, the correlation coefficient of the straight line $R^2 = 0.979$ was achieved. ΔH and ΔS values can be estimated from slope and intercept value of this plot lg K_L vs. $1/T$ and the ΔG values at different temperatures were calculated using the Equation (6), respectively. Table 4 shows the values of thermodynamic parameters of La(III) ions adsorption on SQD-85 resin.

The negative value of ΔG confirms the spontaneity of the adsorption process with increasing temperature, and the positive value of ΔH suggests that the adsorption is endothermic in nature. Although there are no certain criteria related to the ΔH values that define the adsorption type, the heat of adsorption values, which are heats of chemical reactions, are frequently assumed as the comparable values for the chemical

Table 3
Isotherms parameters for the adsorption of La(III) ions by SQD-85 resin

	Langmuir isotherm			Freundlich isotherm		
T (K)	Q_o (mg/g)	K_L (ml/mg)	R^2	n	K_F (mg/g)	R^2
288	468.3	213.5	0.999	12.8	550.8	0.924
298	475.7	215.2	0.999	14.1	587.5	0.895
308	484.0	220.3	0.999	18.5	535.8	0.950

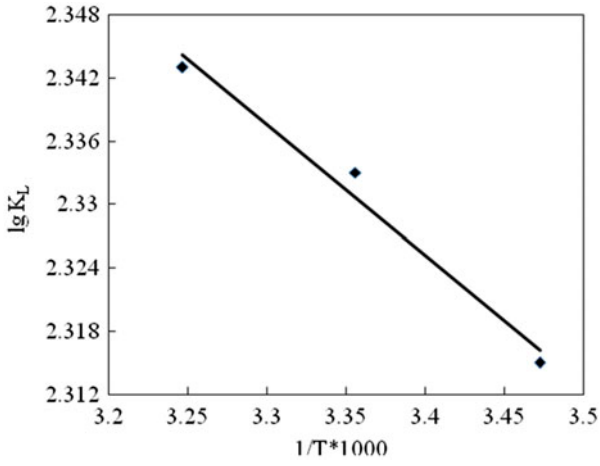

Fig. 3. Influence of temperatures (resin 15.0 mg, 288, 298, and 308 K,100 rpm, and C_0 = 10 mg/30.0 mL).

Table 4
Thermodynamic parameters for La(III) onto SQD-85

		ΔG (kJ/mol)		
ΔH (kJ/mol)	ΔS (J/(K mol))	288 K	298 K	308 K
2.37	52.62	–12.78	–13.31	–13.84

adsorption process. In addition, the values of ΔS were found to be positive due to the exchange of the metal ions with more mobile ions present on the exchanger, which would cause increase in the entropy, during the adsorption process.

3.5. Desorption test

Efficient elution of adsorbed solute from resin is essential to ensure the reuse of resin for repeated adsorption–desorption cycles. To determine the desorption properties of SQD-85 resin for La(III), 15.0 mg resin was added into a mixed solution composed of pH 6.5 buffer solution and desired amount of La (III) solution. After equilibrium reached, the concentration of La(III) in the aqueous phase was determined. Then, the SQD-85 resin separated from aqueous phase was washed three times with pH 6.5 buffer solution. The SQD-85 resin adsorbed La(III) was shaken with 30 mL of varying concentration of HCl. After equilibrium reached, the concentration of La(III) in aqueous phase was determined and then the percentage of elution for La(III) was obtained. The percentages of elution are 97.5, 99.8, 98.9, and 96.1% for 0.5, 1.0, 2.0, and 3.0 mol/L HCl concentration, respectively. The experimental results of elution show that 1.0 mol/L HCl is the most efficient.

3.6. Dynamic adsorption curve

The performance of packed beds is described through the concept of the breakthrough curve. The breakthrough curve shows the loading behavior of La (III) to be removed from solution in a fixed bed and is usually expressed in terms of adsorbed La(III) concentration [C_{ad} = inlet La(III) concentration, (C_0)—outlet La(III) concentration (C_e)] or normalized concentration defined as the ratio of effluent La(III) concentration to inlet La(III) concentration (C_e/C_0) as a function of time or volume of effluent for a given bed height [23]. The area under the breakthrough curve obtained by integrating the adsorbed concentration (C_{ad}; mg/mL) vs. the throughput volume (V; mL) plot can be used to find the total adsorbed La(III) quantity (maximum column capacity). Total adsorbed La(III) quantity (Q; mg/g) in the column for a given feed concentration and flow rate is calculated using the following equation:

$$Q = \int_0^v \frac{(C_0 - C_e)}{m} dV \tag{8}$$

where m (g) is the mass of the adsorbent. The capacity value Q was obtained by graphical integration as 481 mg/g (Fig. 4). Traditionally, the Thomas model is used to fulfill the purpose. The model has the following form [24]:

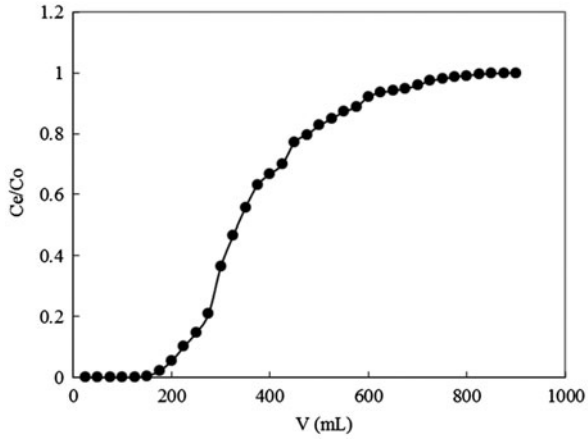

Fig. 4. Experimental breakthrough curve (resin 150 mg, pH 6.5, $C_0 = 0.2$ mg/mL, and flow rate = 0.139 mL/min).

$$\frac{C_e}{C_0} = \frac{1}{1 + \exp[K_T(Q_T m - C_0 V)/\theta]} \tag{9}$$

where K_T (mL/(min mg)) is the Thomas rate constant; and θ (mL/min), the volumetric flow rate. The linearized form of the Thomas model is as follows:

$$\ln\left(\frac{C_0}{C_e} - 1\right) = \frac{K_T Q_T m}{\theta} - \frac{K_T C_0}{\theta} V \tag{10}$$

The kinetic coefficient K_T, and the adsorption capacity of the bed Q_T can be determined from a plot of ln $((C_0/C_e) - 1)$ vs. t at a certain flow rate as shown in Fig. 5. The outlet time t is obtained from V/θ. Thomas equation coefficients for La(III) adsorption were $K_T = 7.5 \times 10^{-3}$ mL/(min mg) and $Q_T = 492$ mg/g. The experimentally observed dynamic sorption capacity (Q, calculated from Equation (8)) was very close to the theoretical predictions saturation adsorption capacity (Q_T) based on Thomas model parameters, which indicates that Thomas model was successfully used for the prediction of the breakthrough curves. Dynamic saturated adsorption amount was larger than the static sorption capacity, due to the contact time of the ion concentration with resins is transitory in the dynamic adsorption process and a high concentration accompanied with SQD-85 resin all along provides a high driving force for the adsorption process.

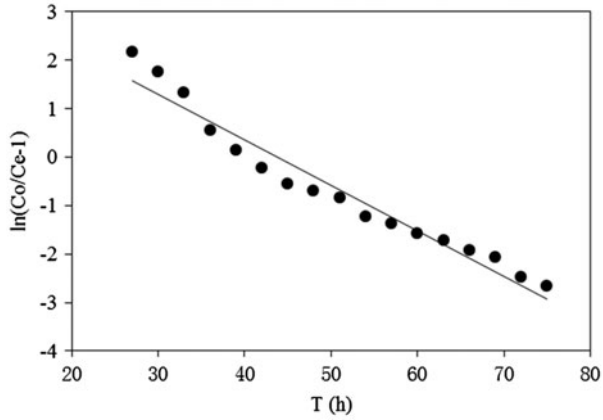

Fig. 5. Linear plots of $\ln(C_0/C_e - 1)$ vs. t by application of Thomas model (resin 150 mg, pH 6.5, $C_0 = 0.2$ mg/mL, and flow rate = 0.139 mL/min).

3.7. Dynamic desorption curve

With respect to the stripping of La(III) from SQD-85 resin, the 1 mol/L HCl eluent was employed. Desorption curve was plotted with the effluent concentration (C_e) vs. elution volume (V) from the column at a certain flow rate. As shown in Fig. 6, the total volume of eluent was 100 mL and the desorption process took 8.3 h, after which further desorption was negligible. Elution volume was significantly less than saturation volume, and desorption capacity was 479.3 mg/g, which was slightly less than the dynamic adsorption capacity. These indicated that elution operation was simple and easy handling, and can obtain a relatively high concentration for economical recovery of La(III).

3.8. Infrared spectra analysis

The FTIR spectral analysis is important to identify some characteristic functional groups which are

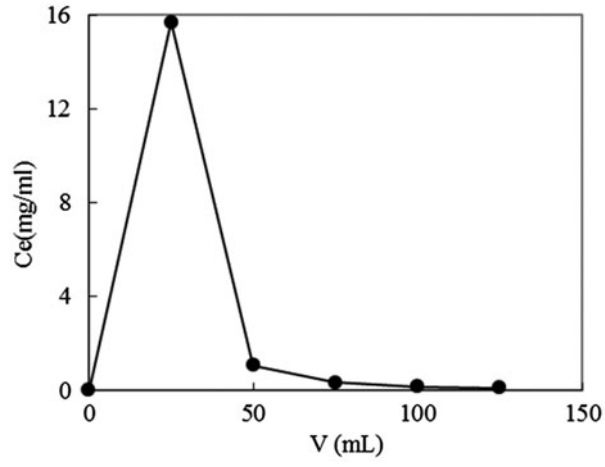

Fig. 6. Dynamic desorption curve (flow rate 0.2 mL/min).

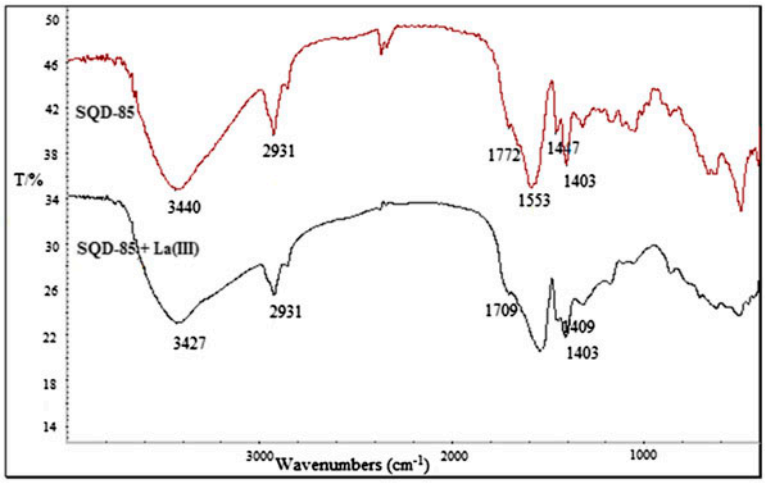

Fig. 7. FTIR spectra of SQD-85 resin before and after being loaded La(III).

responsible of adsorbing metal ion. The information about structural changes caused by the SQD-85 resin loading with La(III) was given by FTIR spectra (Fig. 7). The spectrum of SQD-85 resin showed peaks at 3440 cm^{-1} assigned to stretching vibrations of hydroxyl groups; 2,931 cm^{-1} assigned to the stretching vibrations of $–CH_2$, $–CH_3$ groups; 1,712 cm^{-1} assigned to stretching vibrations of C=O in –COOH groups; 1,403 cm^{-1} assigned to bending vibrations of O–H; 1,553 and 1,447 cm^{-1} assigned to antisymmetric stretching vibration band and symmetric stretching vibration band of –COO– groups, respectively. After the adsorption, the characteristic peak of hydroxyl groups stretching vibrations shifted to lower frequency (from 3,448 to 3,427 cm^{-1}), the peak at 1,709 cm^{-1} decreased in intensity, and 1,403 cm^{-1} was blue-shifted at 1,409 cm^{-1}. These findings may suggest that the hydrogen and oxygen atoms in the –OH and C=O groups were involved in La(III) adsorption. The adsorption mechanism might be partly a result of the ion exchange or complexation between the La(III) ions and carboxyl groups of SQD-85 resin.

4. Conclusions

In this study, batch and column studies for the adsorption of La(III) ions from aqueous solutions have been carried out using SQD-85 resin. The adsorption behavior of SQD-85 for La(III) obeys the Langmuir isotherm better than the Freundlich isotherm. Thermodynamic parameter effects indicate that the adsorption process is spontaneous and endothermic. The La(III) adsorbed on SQD-85 can be eluted by using 1.0 mol/L HCl solution as an eluent. The FTIR spectra of SQD-85 resin before and after the adsorption of La(III) show that hydrogen and oxygen atoms in the –OH and C=O groups are involved in La(III) adsorption. In conclusion, SQD-85 resin can be efficiently used for the removal of La(III) ion from the aqueous solution.

Acknowledgments

The work is supported by the National Natural Science Foundation of China (No. 21276235), PhD Programs Foundation of Ministry of Education of China (No. 20133326110006), and the Key Laboratory of Advanced Textile Materials and Manufacturing Technology (Zhejiang Sci-Tech University), the Ministry of Education (No. 2013006).

References

[1] M.M. Lezhnina, U.H. Kynast, Optical properties of matrix confined species, Opt. Mater. 33 (2010) 4–13.
[2] K. Hantzsche, J. Bohlen, J. Wendt, K.U. Kainer, Effect of rare earth additions on microstructure and texture development of magnesium alloy sheets, Scr. Mater. 63 (2010) 725–730.
[3] J.C.G. Bünzli, A.S. Cha, H.K. Kim, E. Deiters, S.V. Eliseeva, Lanthanide luminescence efficiency in eight- and nine-coordinate complexes: Role of the radiative lifetime, Coord. Chem. Rev. 254 (2010) 2623–2633.
[4] S.Z. Zhang, X.Q. Shau, Speciation of rare earth elements in soil and accumulation by wheat with rare earth fertilizer application, Environ. Pollut. 3 (2011) 395–405.
[5] Y. Kanazawa, M. Kamitani, Rare earth minerals and resources in the world, J. Alloys Compd. 408–412 (2006) 1339–1343.
[6] Ş. Sert, C. Kütahyali, S. İnan, Z. Talip, B. Çetinkaya, M. Eral, Biosorption of lanthanum and cerium from

aqueous solutions by *Platanus orientalis* leaf powder, Hydrometallurgy 90 (2008) 13–18.
[7] M.M. Matlock, B.S. Howerton, D.A. Atwood, Chemical precipitation of heavy metals from acid mine drainage, Water Res. 36 (2002) 4757–4764.
[8] T. Liang, S.M. Ding, W.C. Song, Z.Y. Chong, C.S. Zhang, H.T. Li, A review of fractionations of rare earth elements in plants, J. Rare Earths 26 (2008) 7–15.
[9] K. Kondo, E. Kamio, Separation of rare earth metals with a polymeric microcapsule membrane, Desalination 144 (2002) 249–254.
[10] T. Jeppesen, L. Shu, G. Keir, V. Jegatheesan, Metal recovery from reverse osmosis concentrate, J. Cleaner Prod. 17 (2009) 703–707.
[11] H. Minowa, M. Ebihara, Separation of rare earth elements from scandium by extraction chromatography, Anal. Chim. Acta 498 (2003) 25–37.
[12] C.H. Xiong, C.P. Yao, Preparation and application of acrylic acid grafted polytetrafluoroethylene fiber as a weak acid cation exchanger for adsorption of Er(III), J. Hazard. Mater. 170 (2009) 1125–1132.
[13] S.H. Lin, R.S. Juang, Adsorption of phenol and its derivatives from water using synthetic resins and low-cost natural adsorbents: A review, J. Environ. Manage. 90 (2009) 1336–1349.
[14] N.V. Vlasenko, Y.N. Kochkin, A.V. Topka, P.E. Strizhak, Liquid-phase synthesis of ethyl tert-butyl ether over acid cation-exchange inorganic–organic resins, Appl. Catal. A 362 (2009) 82–87.
[15] X.P. Li, C.P. Yao, C.H. Xiong, J.R. Li, Adsorption of Pb(II) in aqueous solution on SQD-85 resin, Asian J. Chem. 23 (2011) 3387–3392.
[16] E. Pehlivan, T. Altun, The study of various parameters affecting the ion exchange of Cu^{2+}, Zn^{2+}, Ni^{2+}, Cd^{2+}, and Pb^{2+} from aqueous solution on Dowex 50 W synthetic resin, J. Hazard. Mater. 134 (2006) 149–156.
[17] I.G. Shibi, T.S. Anirudhan, Adsorption of Co(II) by a carboxylate-functionalized polyacrylamide grafted lignocellulosics, Chemosphere 58 (2005) 1117–1126.
[18] C.H. Xiong, Sorption of lead(II) in aqueous solution on chitin, Asian J. Chem. 21 (2009) 6005–6014.
[19] G.D. Brykina, T.V. Marchak, L.S. Krysina, T.A. Belyavskaya, Ion sorption of copper and nickel by AV-17X8 anion-exchanger, modified with 1-(2-thiazol ylazo)-2-naphthol-3, 6-disulfonic acid disodium salt, Zh. Anal. Khim. 35 (1980) 2294–2299.
[20] I. Langmuir, The adsorption of gases on plane surfaces of glass, mica, and platinum, J. Am. Chem. Soc. 40 (1918) 1361–1403.
[21] H.M.F. Freundlich, Über die adsorption in lösungen [Over the adsorption in solutions], Z. Physik. Chem. 57 (1906) 385–470.
[22] N. Ünlü, M. Ersoz, Adsorption characteristics of heavy metal ions onto a low-cost biopolymeric sorbent from aqueous solutions, J. Hazard. Mater. 136 (2006) 272–280.
[23] K. Xiao, X.M. Wang, X. Huang, T.D. Waite, X.H. Wen, Analysis of polysaccharide, protein and humic acid retention by microfiltration membranes using Thomas' dynamic adsorption model, J. Membr. Sci. 342 (2009) 22–34.
[24] T. Mathialagan, T. Viraraghavan, Adsorption of cadmium from aqueous solutions by perlite, J. Hazard. Mater. 94 (2002) 291–303.